ACS APPLIED MATERIALS & INTERFACES

Research Article

www.acsami.org

Hybridization between Periodic Mesoporous Organosilica and a Ru(II) Polypyridyl Complex with Phosphonic Acid Anchor Groups

Tatsuto Yui,[†,‡,§] Hiroyuki Takeda,[‡,§,⊥] Yutaro Ueda,[‡] Keita Sekizawa,[‡] Kazuhide Koike,[‡,§,#] Shinji Inagaki,[⊥,§] and Osamu Ishitani*[,‡,§]

[‡]Department of Chemistry, Graduate School of Science and Engineering, Tokyo Institute of Technology, 2-12-1-NE1 O-okayama, Meguro-ku, Tokyo 152-8550, Japan

[⊥]Toyota Central R&D Laboratories Inc., Yokomichi, Nagakute, Aichi 480-1192, Japan

[#]National Institute of Advanced Industrial Science and Technology (AIST), 16-1 Onogawa, Tsukuba, Ibaraki 305-8569, Japan

[§]CREST, Japan Science and Technology Agency (JST), Kawaguchi, Saitama 332-0012, Japan

Supporting Information

ABSTRACT: A new method for the hybridization of a ruthenium(II) polypyridyl complex ($[Ru(bpy)_2((CH_2PO_3H_2)_2\text{-}bpy)]^{2+}$ (**RuP_2^{2+}**: bpy =2,2′-bipyridine; $(CH_2PO_3H_2)_2$-bpy =2,2′-bipyridine-4,4′di(methylphosphonic acid)) with biphenylene-bearing periodic mesoporous organosilica (**Bp−PMO** made from 4,4′bis(triethoxysilyl)biphenyl $[(C_2H_5O)_3Si\text{-}(C_6H_4)_2\text{-}Si(OC_2H_5)_3]$) was developed. Efficient and secure fixation of the ruthenium(II) complex with methylphosphonic acid groups (**RuP_2^{2+}**) in the mesopores of **Bp−PMO** occurred. This method introduced up to 660 μmol of **RuP_2^{2+}** in 1 g of **Bp−PMO**. Two modes of adsorption of **RuP_2^{2+}** in the mesopores of **Bp−PMO** were observed: one is caused by the chemical interaction between the methylphosphonic acid groups of **RuP_2^{2+}** and the silicate moieties of **Bp−PMO** and the other is attributed to aggregation of the **RuP_2^{2+}** complexes. In the case of the former mode, adsorbed **RuP_2^{2+}** (up to 80−100 μmol g^{-1}) did not detach from **Bp−PMO** after washing with acetonitrile, dimethylformamide, or even water. Emission from the excited biphenylene (Bp) units was quantitatively quenched by the adsorbed **RuP_2^{2+}** molecules in cases where more than 60 μmol g^{-1} of **RuP_2^{2+}** was adsorbed, and emission from **RuP_2^{2+}** was observed. Quantitative emission measurements indicated that emission from approximately 100 Bp units can be completely quenched by only one **RuP_2^{2+}** molecule in the mesopore, and photons absorbed by approximately 400 Bp units are potentially accumulated in one **RuP_2^{2+}** molecule.

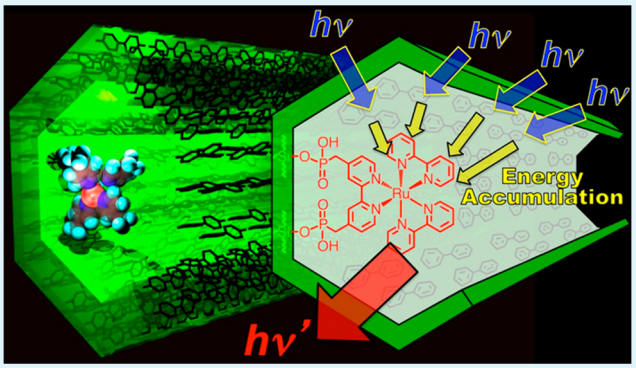

KEYWORDS: *ruthenium complex, periodic mesoporous organosilica, photoinduced energy transfer, methylphosphonic acid group, hybridization, light harvesting*

INTRODUCTION

Hybrids of nanostructured inorganic hosts with organic dyes or metal complexes have attracted much attention because of their unique photochemical and photophysical properties[1−6] such as photochemical stabilization of the incorporated molecules,[7−10] improvement of photoreaction efficiencies and selectivities,[11−13] control of molecular orientations,[14−16] and light-harvesting properties.[17−21]

Periodic mesoporous organosilicas (**PMOs**) are a new type of porous organic/inorganic hybrid materials in which the pore walls have covalently and densely incorporated aligned organic groups within a silica framework.[19,22−25] A number of **PMOs** with various organic groups[24−26] such as biphenylene,[27] pyridine,[28] tetraphenylpyrene,[29] and acridone[30,31] have been synthesized. In particular, the unique photophysical properties of biphenylene-bearing PMO (**Bp−PMO**) with well-ordered mesopores have been thoroughly investigated.[27,32] **Bp−PMO** exhibits strong absorption with a maximum at approximately 270 nm and strongly emits both in the solid state and as a suspension in organic and aqueous solutions. Two hybridization methods for **Bp−PMO** with small molecules have been recently reported: (1) an organosilane precursor with pendant ligands such as 2,2′-bipyridyl units was polymerized with the **Bp−PMO** precursor, i.e., $((H_5C_2O)_3Si\text{-}(C_6H_4)_2\text{-}Si(OC_2H_5)_3)$, in the presence of a surfactant, and then the pendant ligands were coordinated to metal complexes such as $Re(CO)_5Cl$ in the mesopores;[33] (2) **Bp−PMO** and small molecules were mixed together in a solvent containing a surfactant that stabilized the small molecules in the mesopores of **Bp−PMO**.[32,34] Although these methods can result in hybrids with unique properties,

Received: November 11, 2013
Accepted: January 21, 2014
Published: January 21, 2014

   dx.doi.org/10.1021/am405065a | ACS Appl. Mater. Interfaces 2014, 6, 1992−1998

several limitations and disadvantages exist as follows. Synthesis via method 1 requires more time and effort, and the formation of metal complexes in the mesopores of **PMO** is usually low. Because hybrids synthesized by method 2 contain a large amount of surfactant molecules in their mesopores, the diffusion of molecules in the mesopores is potentially much slower compared with that in **PMOs** without the surfactant molecules; this slower diffusion may pose a serious problem for the use of **PMOs** as light-harvesting units for photocatalytic reactions. Another issue with this method is a restriction on the types of solvents that can be used; i.e., the addition of the hybrids synthesized by method 2 in a solvent with a hydroxyl group or groups, such as water and alcohol, readily causes desorption of the metal complexes from the mesopores of **PMOs**.[34]

We report a new method for the synthesis of a hybrid between **Bp−PMO** and a Ru(II) diimine complex with methylphosphonic acid group[13,35−46] ($\mathbf{RuP_2}^{2+}$: Chart 1); this hybrid is very stable, even in various organic solvents and in water. In addition, attractive light-harvesting properties of the hybrid are reported.

Chart 1

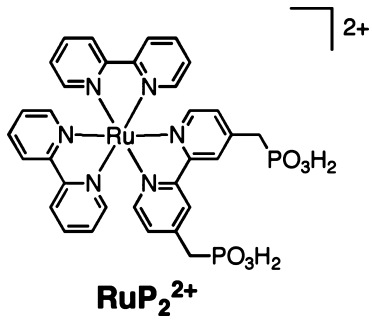

$\mathbf{RuP_2}^{2+}$

EXPERIMENTAL SECTION

Materials. The PF_6^- salts of $[Ru(bpy)_2((CH_2PO_3H_2)_2\text{-bpy})]^{2+}$ ($\mathbf{RuP_2}^{2+}$: bpy = 2,2′-bipyridine; $(CH_2PO_3H_2)_2$-bpy =2,2′-bipyridine-4,4′di(metylphosphonic acid) were synthesized according to the reported methods.[47,48] The synthesis of **Bp−PMO** with a pore diameter of 3.54 nm is reported elsewhere.[27] Molecular weight of **Bp−PMO** was calculated as $-SiO_{1.5}-C_{12}H_8-SiO(OH)-$ (MW = 265.4). Acetonitrile was dried over P_2O_5 three times and then distilled with CaH_2 prior to use.

Synthesis of the Hybrid. **Bp−PMO** powders (2−20 mg) were dispersed in acetonitrile (20−25 mL) containing $\mathbf{RuP_2}^{2+}$ and were subsequently stirred in the dark at room temperature for 14−15 h. The solid was collected by filtration with a PTFE membrane filter (pore size, 0.2 μm, Millipore) and was then washed several times with acetonitrile. The filtrate and acetonitrile used for washing were concentrated, and the volume was adjusted to 5 or 10 mL. The amounts of $\mathbf{RuP_2}^{2+}$ adsorbed in the mesopores of **Bp−PMO** were measured on the basis of the absorbance of the filtrate solution at 465 nm; this absorbance was attributed to the metal-to-ligand charge transfer (^{1}MLCT) absorption of the complex ($\varepsilon = 1.56 \times 10^4$ M^{-1} cm^{-1}). Decomposition of $\mathbf{RuP_2}^{2+}$ was not observed during any of the procedures.

Measurements. Diffuse reflectance UV−vis (DR/UV−vis) absorption spectra of the hybrid powders were recorded on a JASCO V-565 spectrophotometer equipped with an integrating sphere unit (JASCO ISN-469). The longitudinal axes of the spectrum were converted from reflectance (%*R*) to the K/S unit using the Kubelka−Munk function.

The hybrid was dispersed in Ar-saturated acetonitrile (0.05 mg mL^{-1}) by sonication, and the emission spectrum from the hybrid and emission quantum yield (Φ_{em}) were subsequently measured with a multichannel spectrometer attached to a calibrated integrating sphere (C9920−02G: Hamamatsu Photonics) with 266-nm excitation light.[49,50] Φ_{em} of the biphenylene (Bp) unit in **Bp−PMO** and $\mathbf{RuP_2}^{2+}$ were calculated using the emission intensities in the 295−545- and 545−900-nm regions, respectively.

Time-resolved emission spectra were measured with a C4334 Streakscope (Hamamatsu Photonics) using 266 nm excitation (THG pulse of the Spectra-Physics Tsunami Ti:sapphire laser with a Spitfire regenerative amplifier, 35 mW, 1 kHz, fwhm = 150 fs). Emission decay monitored at 420 and 620 nm, which correspond to the emissions from the Bp unit and $\mathbf{RuP_2}^{2+}$, respectively, were measured by the single photon counting method using a FluoroCube 1000U−S spectrofluorometer with 269-nm excitation (1.2 ns fwhm, HORIBA). **Bp−PMO** and the hybrid dispersed in acetonitrile (0.6 mg in 5 mL) were synthesized using the same procedures as those used for the emission spectral measurements. During the measurements, the dispersions were stirred and maintained at 25 °C.

RESULTS AND DISCUSSION

Adsorption of $\mathbf{RuP_2}^{2+}$ in the Mesopores of Bp−PMO. In a typical synthesis of the hybrids, the PF_6^- salt of $\mathbf{RuP_2}^{2+}$ (2×10^{-6} mol) was dissolved in 25 mL of acetonitrile, and then 10 mg of **Bp−PMO** was added to the solution. This suspension was stirred for 14 h at room temperature under dim light. All of the dissolved $\mathbf{RuP_2}^{2+}$ was adsorbed in the mesopores of **Bp−PMO**; therefore, the hybrid with 200 μmol of $\mathbf{RuP_2}^{2+}$ in 1 g of **Bp−PMO** (μmol g^{-1} is the unit henceforth) was obtained. By using this method, various amounts of $\mathbf{RuP_2}^{2+}$ were successfully adsorbed in the mesopores of **Bp−PMO** without the assistance of a surfactant. The relationship between the amount of $\mathbf{RuP_2}^{2+}$ dissolved in the solution and the amount of $\mathbf{RuP_2}^{2+}$ adsorbed in the mesopores of **Bp−PMO** is shown in Figure 1. The

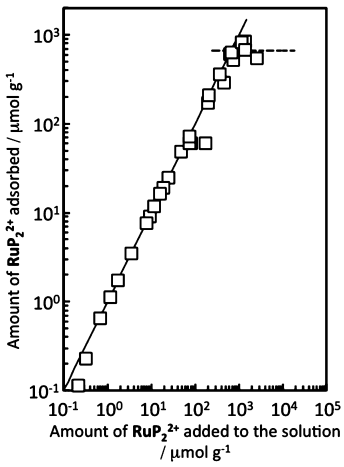

Figure 1. Relationship between the amount of $\mathbf{RuP_2}^{2+}$ dissolved in the solution and the amount of $\mathbf{RuP_2}^{2+}$ adsorbed in the mesopores of **Bp−PMO**. Solid line indicates a quantitative relationship between the loaded and adsorbed $\mathbf{RuP_2}^{2+}$. Dotted line indicates the amount of $\mathbf{RuP_2}^{2+}$ adsorbed at the saturation limit.

dissolved $\mathbf{RuP_2}^{2+}$ was quantitatively adsorbed in the mesopores of **Bp−PMO** up to 500 μmol g^{-1}; however, the amount adsorbed was saturated at higher amounts of $\mathbf{RuP_2}^{2+}$. The maximum amount of $\mathbf{RuP_2}^{2+}$ adsorbed was 665 ± 127 μmol g^{-1}. Because, in contrast, $[Ru(dmb)_3]^{2+}$ (dmb =4,4′-dimethyl-2,2′-bipyridine) without the phosphonate groups could not be

adsorbed in the mesopores of **Bp−PMO**, the methylphosphonic acid group are expected to function as a useful anchor.

The total length of the mesopores of **Bp−PMO** (5.4×10^{19} nm g^{-1}) can be calculated as the pore volume (0.49 cm^3 g^{-1})[33] divided by the cross-sectional area of a hexagonal pore (9.09 nm^2).[34] Under the maximum adsorption condition (660 μmol g^{-1}), the average number of RuP_2^{2+} molecules adsorbed in a mesopore of **Bp−PMO** with a length of 10 nm was determined to be 72; the maximum occupied volume for both RuP_2^{2+} and the counteranion PF_6^-, which were assumed to be spheres with diameters 1.4 and 0.4 nm, respectively, were estimated to be 113 and 5% of the space in the mesopores of **Bp−PMO**,[33,34] respectively, if RuP_2^{2+} is assumed be adsorbed only inside the mesopore. This estimation indicates that the space in the mesopore is almost fully occupied by $RuP_2^{2+}(PF_6^-)_2$.

When the hybrid RuP_2^{2+}**−Bp−PMO** powders with various amounts of RuP_2^{2+} were redispersed in acetonitrile and dimethylformamide under 14 h of stirring, no desorption of RuP_2^{2+} was observed. However, when the hybrid was redispersed in water, a portion of RuP_2^{2+} was desorbed, and 80−100 μmol g^{-1} of RuP_2^{2+} remained in the mesopores of **Bp−PMO**. The RuP_2^{2+} remaining in the pores was not desorbed by repetitive washing with water. These results suggest that two adsorption mechanisms govern the adsorption of RuP_2^{2+} in the mesopores of **Bp−PMO**. Stronger adsorption (ca. 80−100 μmol g^{-1} of RuP_2^{2+}, no desorption with water) is expected to result from direct interaction of the methylphosphonic acid group with surface silanol (Si−OH) groups of **Bp−PMO**; the surface of **Bp−PMO** has been reported to contain [Si−OH] of 3.77 mmol g^{-1}.[27] However, weaker adsorption of RuP_2^{2+} might be caused by the aggregation of the RuP_2^{2+} molecules, which are desorbed from the mesopores of **Bp−PMO** by washing with water. The amounts of silanol groups were much larger even compared to the maximum amount of the adsorbed RuP_2^{2+}. This is reasonable because the size of the complex is much larger than the silanol group and many silanol groups are densely populated on the walls of mesopores. Most of silanol groups should not be able to interact with the methylphosphonic acids groups of RuP_2^{2+}.

Two typical DR/UV−vis spectra of the hybrids with different amounts of adsorbed RuP_2^{2+} are shown in Figure 2: black and red lines indicate the spectra of a saturated sample (639 μmol g^{-1}) and a lower-adsorbed sample (48 μmol g^{-1}), respectively. In the inset figure, absorption spectrum of RuP_2^{2+} in MeCN is also shown. Distinct broadening was observed in the case of the saturated hybrid (inset of Figure 2). This difference indicates that the adsorbed RuP_2^{2+} molecules were well-dispersed in the hybrid with the lower amount of adsorbed RuP_2^{2+}, whereas the RuP_2^{2+} molecules strongly interacted with each other in the case of **Bp−PMO** saturated with RuP_2^{2+}. Moreover, Φ_{em} measurements indicated that the hybrid with a higher amount of adsorbed RuP_2^{2+} exhibited lower emission intensity because of the formation of RuP_2^{2+} aggregates, which are self-quenching, as will be discussed later.

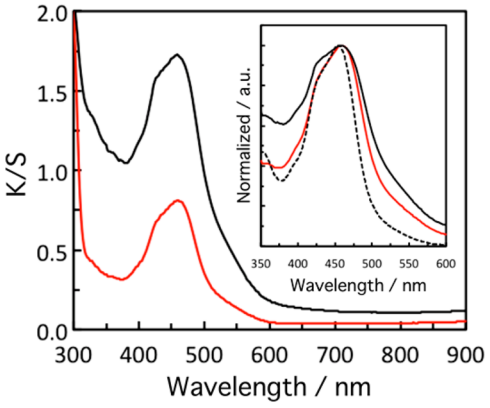

Figure 2. Diffuse reflectance UV−vis (DR/UV−vis) absorption spectra of the hybrids with low (48 μmol g^{-1}, red line) and high (639 μmol g^{-1}, black line) amounts of adsorbed RuP_2^{2+}. Inset shows the normalized spectra of the ^{1}MLCT band of the hybrid and RuP_2^{2+} in MeCN solution (dotted line) .

Therefore, most of the RuP_2^{2+} molecules can be concluded to interact with the surface Si−OH groups of **Bp−PMO** in the case of low adsorption (80−100 μmol g^{-1}). However, higher adsorption induces the aggregation of RuP_2^{2+} in the mesopores.

Light Harvesting. Energy transfer phenomena from the excited Bp unit to the RuP_2^{2+} adsorbed in the mesopores of **Bp−PMO** were investigated via emission measurements of the hybrid dispersed in acetonitrile using 266 nm excitation light. Based on the spectral overlap between the absorption of RuP_2^{2+} in MeCN solution and the emission from Bp unit, the Forster radii for energy transfer from the excited Bp-PMO to RuP_2^{2+} was calculated as 3.2 nm.[34] In the absence of RuP_2^{2+} (i.e., **Bp−PMO** alone), strong emission from the Bp units was observed at 300−450 nm with $\Phi_{em} = 0.500 \pm 0.005$.[32,34] The adsorption of RuP_2^{2+} in the mesopores of **Bp−PMO** caused emission quenching from the Bp units, and a new broad emission (λ_{max} = 620 nm) from the ^{3}MLCT excited state of RuP_2^{2+} appeared (Figure 3). With the adsorption of additional

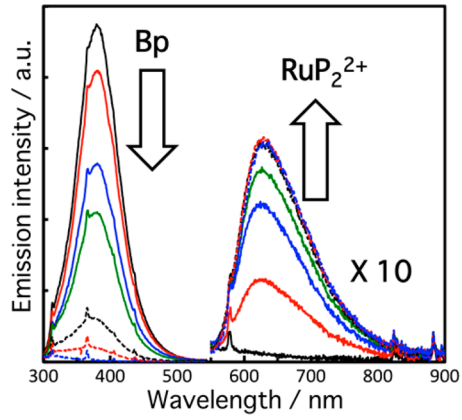

Figure 3. Emission spectra of **Bp−PMO** (black solid line) and the hybrids with various amounts of RuP_2^{2+} adsorbed (3.5, 7.7, 12, 25, 60, and 290 μmol g^{-1}) in Ar-saturated acetonitrile dispersions. The emission intensities were corrected according to the absorbance at the excitation wavelength (266 nm) .

RuP_2^{2+} up to 60 μmol g^{-1}, weaker emission from the Bp units and stronger emission from RuP_2^{2+} were observed, as shown in Figure 4. Almost no emission from the Bp unit was observed with more than 60 μmol g^{-1} of RuP_2^{2+}. The incident light is primarily absorbed by the Bp units even in the saturated condition of RuP_2^{2+} (660 μmol g^{-1}) in the hybrid because the absorbance ratio between the Bp units and RuP_2^{2+} is 89:11 if both the Bp units and the RuP_2^{2+} are homogeneously dispersed in the solution ($\varepsilon_{266\ nm}$ (precursor of **Bp−PMO**)[34] = 2.66×10^4 $M^{-1}cm^{-1}$ and $\varepsilon_{266\ nm}$ (RuP_2^{2+}) = 1.86×10^4 M^{-1} cm^{-1}). When the amount of RuP_2^{2+} adsorbed was between 60 and 80 μmol

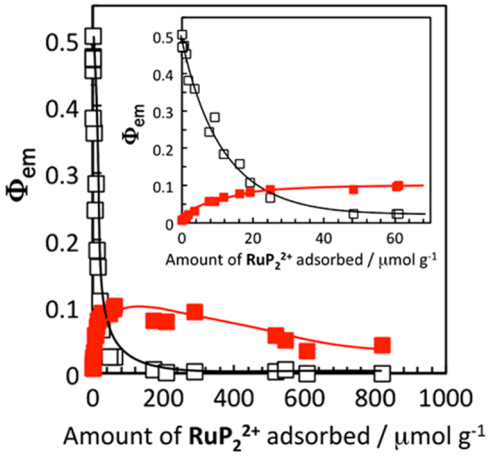

Figure 4. Emission quantum yields (Φ_{em}) of the Bp units (open squares) and $\mathbf{RuP_2^{2+}}$ (red squares) in the hybrids with various amounts of adsorbed $\mathbf{RuP_2^{2+}}$ in acetonitrile. The same plots corresponding to the lower adsorption region are presented in the inset.

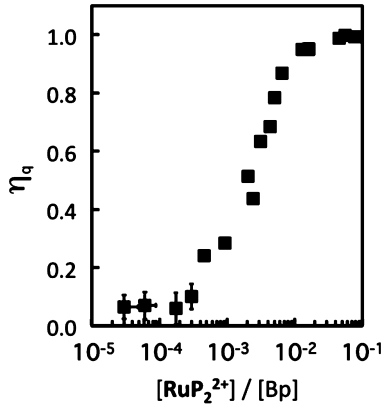

Figure 5. Quenching efficiencies of the excited Bp unit by $\mathbf{RuP_2^{2+}}$ (η_q) at various $[\mathbf{RuP_2^{2+}}]/[Bp]$ ratios. The internal filter effect of $\mathbf{RuP_2^{2+}}$ was excluded by the absorbance ratio between the Bp units and $\mathbf{RuP_2^{2+}}$ (see text).

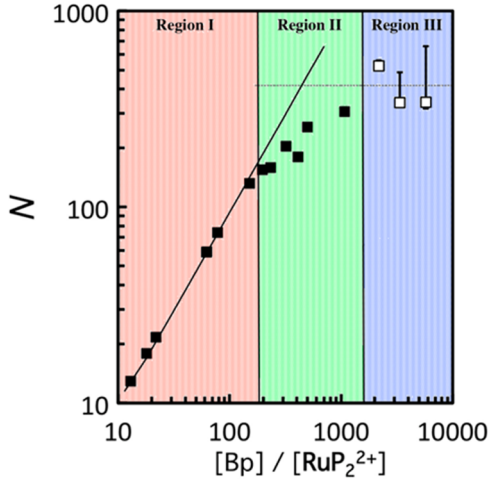

Figure 6. Relationship between molar ratio of the Bp units and adsorbed $\mathbf{RuP_2^{2+}}$ ($[Bp]/[\mathbf{RuP_2^{2+}}]$) and the number of quenched excited Bp units (N).

$\mathbf{g^{-1}}$ (the ratio of the absorption of photons between by the Bp units and $\mathbf{RuP_2^{2+}}$ was between 98.9: 1.1 and 98.5: 1.5), Φ_{em} from $\mathbf{RuP_2^{2+}}$ in **Bp−PMO** reached 0.1, which is similar to the yield achieved from both $\mathbf{RuP_2^{2+}}$ in a homogeneous acetonitrile solution and $\mathbf{RuP_2^{2+}}$ adsorbed onto Al_2O_3 powder in nonaggregated form (i.e., 5 μmol g^{-1}). The emission quenching and energy transfer phenomena indicate that energy transfer from the excited Bp unit to $\mathbf{RuP_2^{2+}}$ proceeded quantitatively in the hybrid. When the amount of $\mathbf{RuP_2^{2+}}$ adsorbed exceeded ~100 μmol g^{-1}, Φ_{em} of $\mathbf{RuP_2^{2+}}$ in **Bp−PMO** gradually decreased (Figure 4) because of self-quenching between the closely packed $\mathbf{RuP_2^{2+}}$ molecules in the mesopores of **Bp−PMO**. Under such conditions, broadening of the ^{1}MLCT absorption band was observed, as previously described. The self-quenching behavior was also detected by emission lifetime analysis, as will be described latter.

Energy-transfer efficiencies (η_{ENT}) from the excited Bp unit to the adsorbed $\mathbf{RuP_2^{2+}}$ in the mesopore could be calculated by eq 1 in the case of hybrids with less than 80 μmol g^{-1} of adsorbed $\mathbf{RuP_2^{2+}}$ because quenching of the excited Bp unit quantitatively produced the excited $\mathbf{RuP_2^{2+}}$ as described above.

$$\eta_{ENT} \approx \eta_q = (\Phi_{Bp} - \Phi_{Hybrid})/\Phi_{Bp} \quad (1)$$

where η_q is the quenching efficiency of the excited Bp unit by $\mathbf{RuP_2^{2+}}$ and Φ_{Hybrid} and Φ_{Bp} indicate Φ_{em} from the Bp units with and without the adsorption of $\mathbf{RuP_2^{2+}}$, respectively. A relationship between η_q and the molar ratio of $\mathbf{RuP_2^{2+}}$ units to Bp units ($[\mathbf{RuP_2^{2+}}]/[Bp]$) is shown in Figure 5, where [Bp] and $[\mathbf{RuP_2^{2+}}]$ are the numbers of Bp molecules and adsorbed $\mathbf{RuP_2^{2+}}$ molecules in the hybrid, respectively. An increase in $[\mathbf{RuP_2^{2+}}]/[Bp]$ resulted in larger η_q, and emission from the Bp units was quantitatively quenched in the cases of $[\mathbf{RuP_2^{2+}}]/[Bp] > 0.01$ (> 60 μmol g^{-1}); i.e., the $\mathbf{RuP_2^{2+}}$ adsorbed in the mesopores completely quench the emission from 100 Bp units located around one $\mathbf{RuP_2^{2+}}$ molecule.

Equation 2 gives the number of excited Bp units that can potentially transfer excitation energy to one $\mathbf{RuP_2^{2+}}$ (N).[34]

$$N = ([Bp]/[\mathbf{RuP_2^{2+}}])\eta_q \quad (2)$$

The relationship between $[Bp]/[\mathbf{RuP_2^{2+}}]$ and N is shown in Figure 6, where emission quenching behaviors can be classified into three regions. In region I, good fitting of the data to the solid line with slope =1 suggests $\eta_q = 1$, i.e., emission from the Bp units is completely quenched ($[Bp]/[\mathbf{RuP_2^{2+}} < 100$), as previously described. Lower amounts of $\mathbf{RuP_2^{2+}}$ adsorbed in the mesopores of **Bp−PMO** resulted in leakage of emission from the Bp unit (region II). Finally, N reached a constant value, i.e., 403 ± 86 (region III). These results indicate that, in Region III, $\mathbf{RuP_2^{2+}}$ molecules are sufficiently isolated from each other and that each molecule can accept excitation energy from approximately 400 Bp units.

A relationship between the radius of a virtual sphere (R) with $\mathbf{RuP_2^{2+}}$ at the center, which is postulated to be located 1.5 nm from the wall, and the number of Bp units (N_{calc}) within this virtual sphere is shown in Figure S1 in the Supporting Information.[34] On the basis of this estimation, the radius of the virtual sphere in which the Bp units (ca. 400 units) can transfer excitation energy to one $\mathbf{RuP_2^{2+}}$ molecule is calculated as 3.3 nm.

Time-Resolved Emission Analysis. Time-resolved emission spectra of **Bp−PMO** and $\mathbf{RuP_2^{2+}}$**−Bp−PMO** in acetonitrile were measured using 266 nm excitation light. In

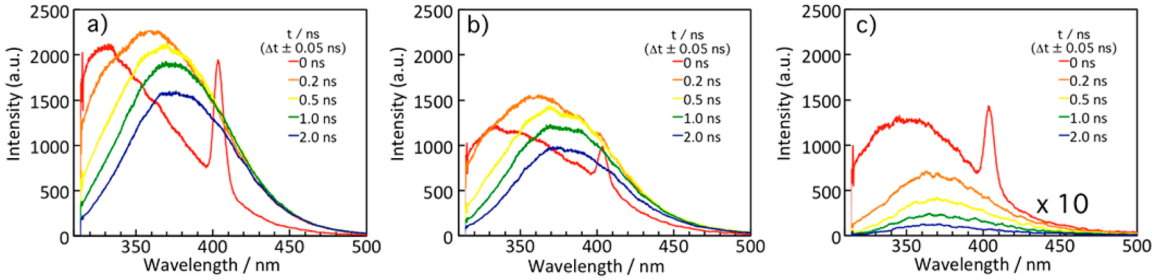

Figure 7. Time-resolved emission spectra of (a) **Bp−PMO** and the hybrid with (b) 1.7 and (c) 172 μmol g^{-1} of $\mathbf{RuP_2^{2+}}$ dispersed in acetonitrile at room temperature. The emission intensity in c was multiplied by 10. The sharp peaks at 405 nm in the spectra measured just after excitation were attributed to the scattering of the excitation laser radiation.

the case of **Bp−PMO**, fluorescence with an emission maximum at 330 nm was observed immediately after excitation (Figure 7a, red line). The peak position was shifted to longer wavelengths of up to 380 nm over time. This shift is consistent with the reported emission behaviors of powdered **Bp−PMO**:[51] the lowest singlet excited state (S_1) of the Bp unit was produced within 50 ps, which was followed by interactions with another Bp unit to give three types of excimers within 200 ps after excitation. Emission from the excimers decayed within 27 ns. In the case of the hybrid with 20 μmol g^{-1} of $\mathbf{RuP_2^{2+}}$ (Figure 7b), quenching of S_1 was observed; this weaker S_1 was likely caused by the transfer of energy to the adsorbed $\mathbf{RuP_2^{2+}}$ in the mesopores of **Bp−PMO**. In the case of the hybrid with 170 μmol g^{-1} of $\mathbf{RuP_2^{2+}}$ (Figure 7c), S_1 was not observed, and only weak excimer emission was observed because of the more efficient energy transfer process. In this case, the excimer emission rapidly decreased within 200 ps after excitation, and an increase in the emission from the $\mathbf{RuP_2^{2+}}$ was observed with a similar rate constant. This increased emission is expected to be caused by the rapid energy transfer from the three types of excimers to $\mathbf{RuP_2^{2+}}$.

The emission decay profile of the adsorbed $\mathbf{RuP_2^{2+}}$ was monitored at 625 nm after excitation of the hybrid at 266 nm. A typical example (12 μmol g^{-1} of $\mathbf{RuP_2^{2+}}$) is shown in Figure 8,

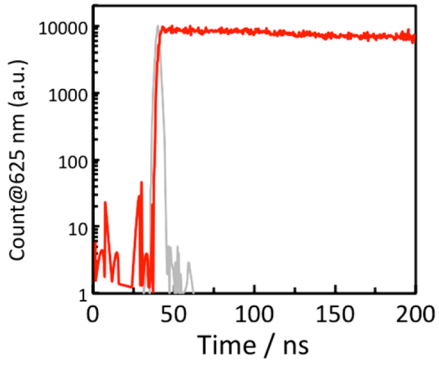

Figure 8. Emission decay profiles of the hybrid with 12 μmol g^{-1} of $\mathbf{RuP_2^{2+}}$ at 625 nm in acetonitrile. Gray line indicates apparatus response.

where the $\mathbf{RuP_2^{2+}}$ molecule was independently adsorbed in the mesopores of **Bp−PMO**. The decay profile could be fitted with a single exponential function, and the lifetime was 902 ns, which was similar to those measured from both homogeneous acetonitrile solution of $\mathbf{RuP_2^{2+}}$ and $\mathbf{RuP_2^{2+}}$ adsorbed onto Al_2O_3 particles. However, in the case of the higher adsorbed sample (172 μmol g^{-1}), we fitted the emission from $\mathbf{RuP_2^{2+}}$ with a double exponential function, and the lifetimes were 13 and 902 ns. The additional fast decay should be induced by the self-quenching due to the formation of $\mathbf{RuP_2^{2+}}$ aggregates in the mesopores (Figures 2 and 4).

All of the emission decay profiles of the three different excimers (E_1, E_2, and E_3) from the Bp units were monitored at 370 nm and were reasonably fitted with three exponential functions (eq 3 and Table 1)[51]

$$I(t) = \sum_{n=1}^{3} A_n e^{-t/\tau_n} \quad (3)$$

Table 1. Emission Lifetimes of the Excimers of the Bp units in Bp−PMO and the Hybrids with Various Amounts of Adsorbed $\mathbf{RuP_2^{2+}}$

amount of $\mathbf{RuP_2^{2+}}$ adsorbed (μmol g^{-1})	emission lifetime at 370 nm (ns) (A_n^{rel} (%))		
	τ_1	τ_2	τ_3
0	0.658 ± 0.004 (25)	10.00 ± 0.19 (33)	28.26 ± 0.08 (42)
1.7	0.861 ± 0.003 (43)	9.86 ± 0.12 (37)	25.35 ± 0.10 (21)
12	0.510 ± 0.003 (58)	3.63 ± 0.05 (33)	11.79 ± 0.11 (9)
25	0.527 ± 0.003 (60)	3.70 ± 0.05 (31)	11.55 ± 0.11 (9)
170	0.279 ± 0.002 (83)	1.71 ± 0.03 (14)	13.20 ± 0.06 (4)

where $I(t)$, A_n, and τ_n (n = 1−3) are the emission intensities, pre-exponential factors, and the emission lifetimes, respectively. Figure 9 shows the emission decay profiles of both **Bp−PMO** and the hybrid with 170 μmol g^{-1} of $\mathbf{RuP_2^{2+}}$ as typical examples. In the case of **Bp−PMO**, the emission decayed with lifetimes of 0.7 ns, 10.0 ns, and 28.3 ns; these lifetimes are similar to the emission lifetimes reported for three kinds of excimers measured for powdered **Bp−PMO**.[51] The fluorescence from S_1 of the monomeric Bp unit was reasonably assumed to not be detected because of the weak emission from S_1 at 370 nm.[51]

The emission-decay rate constants from hybrids with various amounts of adsorbed $\mathbf{RuP_2^{2+}}$ are summarized in Table 1. These results also strongly indicate that $\mathbf{RuP_2^{2+}}$ efficiently quenched the excited state of the Bp units. Figure 10 shows the relationships between lifetime (τ_n) and proportion of the pre-exponential function (A_n^{rel}) in the hybrids with various adsorbed amounts of $\mathbf{RuP_2^{2+}}$, which was calculated using eq 4.

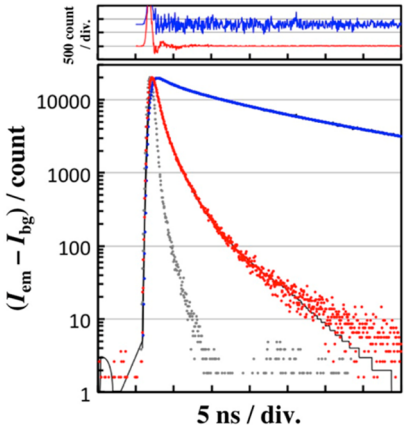

Figure 9. Decay profiles of **Bp−PMO** (blue) and the hybrid with 170 μmol g^{-1} of $\mathbf{RuP_2^{2+}}$ (red) at 370 nm in acetonitrile. Gray dots indicate apparatus response. Excitation wavelength was 269 nm.

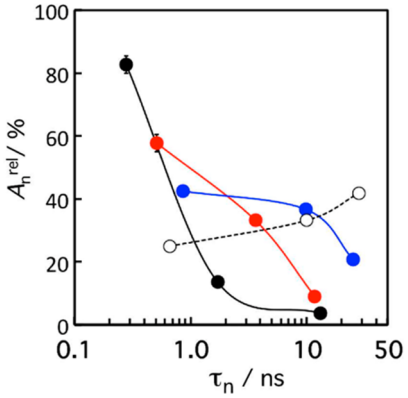

Figure 10. Relationships between lifetimes (τ_n) and proportion of the pre-exponential function (A_n^{rel}) of the hybrids with various adsorbed amounts of $\mathbf{RuP_2^{2+}}$: (white circles) 0, (blue circles) 1.7, (red circles) 12, and (black circles) 170 μmol g^{-1}.

$$A_n^{rel} = \frac{A_n}{\sum_{n=1}^{3} A_n} \times 100 \quad (4)$$

Each emission lifetime of the excimers was shortened as the amount of adsorbed $\mathbf{RuP_2^{2+}}$ increased. A_n^{rel} of the longest component decreased with increasing amount of $\mathbf{RuP_2^{2+}}$ adsorbed, whereas that of the shortest component drastically increased. These results indicate that the adsorbed $\mathbf{RuP_2^{2+}}$ could quench all of the excited states of the three excimers of the Bp units.

On the basis of these results, the energy transfer phenomena from the excited Bp units to the adsorbed $\mathbf{RuP_2^{2+}}$ are schematically drawn in Figure 11. As shown in Figure 11a, one $\mathbf{RuP_2^{2+}}$ molecule accepts excitation energy from approximately 400 Bp units, and the longest quenchable radius was estimated to be 3.3 nm. In the case of a low amount of adsorbed $\mathbf{RuP_2^{2+}}$ (region I in Figure 6), each $\mathbf{RuP_2^{2+}}$ potentially quenches approximately 400 neighboring excited Bp units; however, emission from the other distant Bp units is "leaked" (Figure 11b). With an increase in the amount of adsorbed $\mathbf{RuP_2^{2+}}$ (region II), emission from additional Bp units is quenched, whereas the areas quenched by $\mathbf{RuP_2^{2+}}$ overlap each other, and some emission from the Bp units is still observed (Figure 11c). In the case of Figure 11d (regions III), all of the Bp units are covered with the quenchable area of $\mathbf{RuP_2^{2+}}$ and

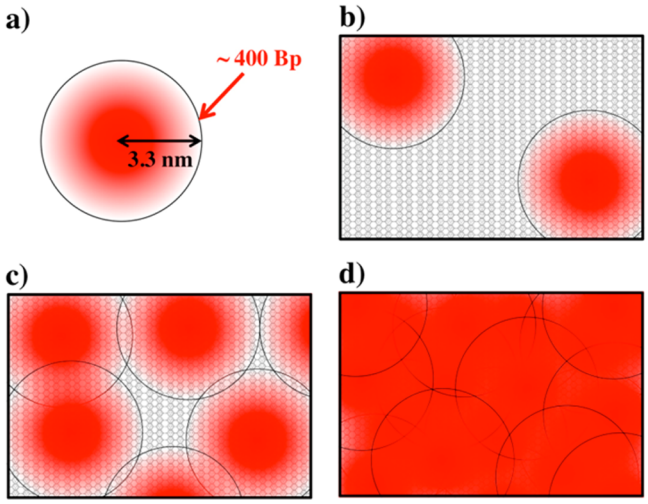

Figure 11. Quenching behavior of the excited Bp units induced by the adsorbed $\mathbf{RuP_2^{2+}}$ in the mesopores. (a) Quenchable radius by one $\mathbf{RuP_2^{2+}}$ molecule and the number of Bp units in the radius. (b−d) Quenchable areas in the cases of regions I, II, and III in Figure 6. All illustrations are drawn two-dimensionally for simplification.

emission from the Bp units is completely quenched by $\mathbf{RuP_2^{2+}}$. Therefore, in this case, additional adsorption of $\mathbf{RuP_2^{2+}}$ no longer increases the emission intensity of the absorbed $\mathbf{RuP_2^{2+}}$.

CONCLUSION

A Ru(II) trisdiimine complex with methylphosphonic acid groups was successfully introduced and strongly adsorbed in the mesopores of **Bp−PMO**. Because this method does not require the use of any assistant reagents such as a surfactant, it is potentially applicable to the adsorption of various photofunctional molecules such as metal-complex photocatalysts in various types of PMOs. Emission from Bp units in the **Bp−PMO** framework was efficiently quenched by $\mathbf{RuP_2^{2+}}$ in the mesopores of **Bp−PMO**, and the excited state of $\mathbf{RuP_2^{2+}}$ was quantitatively produced. Emission from approximately 100 neighboring Bp units was completely quenched by only one $\mathbf{RuP_2^{2+}}$, and energy absorbed by approximately 400 Bp units was potentially transferred to one neighboring $\mathbf{RuP_2^{2+}}$. This hybridization method is applicable for developing a novel type of artificial photosynthesis, which is currently underway in our laboratory.

ASSOCIATED CONTENT

Supporting Information

Plot of the number of Bp units (N_{calc}) inside of a virtual sphere (R). This material is available free of charge via the Internet at http://pubs.acs.org/.

AUTHOR INFORMATION

Corresponding Author

*E-mail: ishitani@chem.titech.ac.jp.

Present Address

†T.Y. is currently at Department of Materials Science and Technology, Faculty of Engineering, and Center for Transdisciplinary Research, Niigata University, 8050 Ikarashi-2, Niigata 950−2181, Japan

Notes

The authors declare no competing financial interest.

■ ACKNOWLEDGMENTS

This work was partly supported by the Next Generation World-Leading Researchers Funding Program (NEXT Program) and All Nippon Artificial Photosynthesis Project for Living Earth (AnApple) of JSPS.

■ REFERENCES

(1) Ogawa, M.; Kuroda, K. *Chem. Rev.* **1995**, *95*, 399−438.
(2) Shichi, T.; Takagi, K. *J. Photochem. Photobiol. C: Photochem. Rev.* **2000**, *1*, 113−130.
(3) Ogawa, M. *J. Photochem. Photobiol. C: Photochem. Rev.* **2002**, *3*, 129−146.
(4) Tachikawa, T.; Yui, T.; Fujitsuka, M.; Takagi, K.; Majima, T. *Chem. Lett.* **2005**, *34*, 1522−1523.
(5) Takagi, S.; Eguchi, M.; Tryk, D. A.; Inoue, H. *J. Photochem. Photobiol. C: Photochem. Rev.* **2006**, *7*, 104−126.
(6) Yui, T.; Takagi, K. In *Bottom-up Nanofabrication*; Ariga, K., Nalwa, H. S., Eds.; American Scientific Publishers: Valencia, CA, 2009; Vol. 5, p 35−90.
(7) Miyamoto, N.; Kuroda, K.; Ogawa, M. *J. Phys. Chem. B* **2004**, *108*, 4268−4274.
(8) Yui, T.; Kobayashi, Y.; Yamada, Y.; Tsuchino, T.; Yano, K.; Kajino, T.; Fukushima, Y.; Torimoto, T.; Inoue, H.; Takagi, K. *Phys. Chem. Chem. Phys.* **2006**, *8*, 4585−4590.
(9) Miyamoto, N.; Yamada, Y.; Koizumi, S.; Nakato, T. *Angew. Chem., Int. Ed.* **2007**, *46*, 4123−4127.
(10) Yui, T.; Kobayashi, Y.; Yamada, Y.; Yano, K.; Fukushima, Y.; Torimoto, T.; Takagi, K. *ACS Appl. Mater. Interfaces* **2011**, *3*, 931−935.
(11) Usami, H.; Takagi, K.; Sawaki, Y. *J. Chem. Soc., Perkin Trans. 2* **1990**, 1723−1728.
(12) Takagi, K.; Shichi, T.; Usami, H.; Sawaki, Y. *J. Am. Chem. Soc.* **1993**, *115*, 4339−4344.
(13) Maeda, K.; Sekizawa, K.; Ishitani, O. *Chem. Commun.* **2013**, *49*, 10127−10129.
(14) Sasai, R.; Shin'ya, N.; Shichi, T.; Takagi, K.; Gekko, K. *Langmuir* **1999**, *15*, 413−418.
(15) Eguchi, M.; Takagi, S.; Inoue, H. *Chem. Lett.* **2006**, *35*, 14−15.
(16) Itoh, T.; Shichi, T.; Yui, T.; Takagi, K. *Langmuir* **2005**, *21*, 3217−3220.
(17) Yui, T.; Kameyama, T.; Sasaki, T.; Torimoto, T.; Takagi, K. *J. Porphyrins Phthalocyanines* **2007**, *11*, 428−433.
(18) Ishida, Y.; Shimada, T.; Masui, D.; Tachibana, H.; Inoue, H.; Takagi, S. *J. Am. Chem. Soc.* **2011**, *133*, 14280−14286.
(19) Hoffmann, F.; Froba, M. *Chem. Soc. Rev.* **2011**, *40*, 608−620.
(20) Rao, K. V.; Datta, K. K. R.; Eswaramoorthy, M.; George, S. J. *Chem.—Eur. J.* **2012**, *18*, 2184−2194.
(21) Calzaferri, G. *Langmuir* **2012**, *28*, 6216−6231.
(22) Inagaki, S.; Guan, S.; Fukushima, Y.; Ohsuna, T.; Terasaki, O. *J. Am. Chem. Soc.* **1999**, *121*, 9611−9614.
(23) Inagaki, S.; Guan, S.; Ohsuna, T.; Terasaki, O. *Nature* **2002**, *416*, 304−307.
(24) Tani, T.; Mizoshita, N.; Inagaki, S. *J. Mater. Chem.* **2009**, *19*, 4451−4456.
(25) Kapoor, M. P.; Inagaki, S. In *Bottom-up Nanofabrication*; Ariga, K., Nalwa, H. S., Eds.; American Scientific Publishers: Stevenson Ranch, CA, 2009; Vol. 6, pp 255−281.
(26) Mizoshita, N.; Tani, T.; Inagaki, S. *Chem. Soc. Rev.* **2011**, *40*, 789−800.
(27) Kapoor, M. P.; Yang, Q.; Inagaki, S. *J. Am. Chem. Soc.* **2002**, *124*, 15176−15177.
(28) Waki, M.; Mizoshita, N.; Ohsuna, T.; Tani, T.; Inagaki, S. *Chem. Commun.* **2010**, *46*, 8163−8165.
(29) Mizoshita, N.; Goto, Y.; Maegawa, Y.; Tani, T.; Inagaki, S. *Chem. Mater.* **2010**, *22*, 2548−2554.
(30) Takeda, H.; Goto, Y.; Maegawa, Y.; Ohsuna, T.; Tani, T.; Matsumoto, K.; Shimada, T.; Inagaki, S. *Chem. Commun.* **2009**, 6032−6034.
(31) Maegawa, Y.; Mizoshita, N.; Tani, T.; Inagaki, S. *J. Mater. Chem.* **2010**, *20*, 4399−4403.
(32) Inagaki, S.; Ohtani, O.; Goto, Y.; Okamoto, K.; Ikai, M.; Yamanaka, K.-i.; Tani, T.; Okada, T. *Angew. Chem., Int. Ed.* **2009**, *48*, 4042−4046.
(33) Takeda, H.; Ohashi, M.; Tani, T.; Ishitani, O.; Inagaki, S. *Inorg. Chem.* **2010**, *49*, 4554−4559.
(34) Yamamoto, Y.; Takeda, H.; Yui, T.; Ueda, Y.; Koike, K.; Inagaki, S.; Ishitani, O. *Chem. Sci.* **2014**, *5*, 639−648.
(35) Yan, S. G.; Hupp, J. T. *J. Phys. Chem.* **1996**, *100*, 6867−6870.
(36) Zaban, A.; Ferrere, S.; Gregg, B. A. *J. Phys. Chem. B* **1998**, *102*, 452−460.
(37) Will, G.; Boschloo, G.; Rao, S. N.; Fitzmaurice, D. *J. Phys. Chem. B* **1999**, *103*, 8067−8079.
(38) Will, G.; Sotomayor, S.; Nagaraja Rao, J.; Fitzmaurice, D. *J. Mater. Chem.* **1999**, *9*, 2297−2299.
(39) Merrins, A.; Kleverlaan, C.; Will, G.; Rao, S. N.; Scandola, F.; Fitzmaurice, D. *J. Phys. Chem. B* **2001**, *105*, 2998−3004.
(40) Terada, K.; Kobayashi, K.; Haga, M.-a. *Dalton Trans.* **2008**, 4846−4854.
(41) Elliott, K. J.; Harriman, A.; Le Pleux, L.; Pellegrin, Y.; Blart, E.; Mayer, C. R.; Odobel, F. *Phys. Chem. Chem. Phys.* **2009**, *11*, 8767−8773.
(42) Odobel, F.; SÈverac, M.; Pellegrin, Y.; Blart, E.; Fosse, C.; Cannizzo, C.; Mayer, C. R.; Elliott, K. J.; Harriman, A. *Chem.—Eur. J.* **2009**, *15*, 3130−3138.
(43) Concepcion, J. J.; Jurss, J. W.; Hoertz, P. G.; Meyer, T. J. *Angew. Chem., Int. Ed.* **2009**, *48*, 9473−9476.
(44) Brennaman, M. K.; Patrocinio, A. O. T.; Song, W.; Jurss, J. W.; Concepcion, J. J.; Hoertz, P. G.; Traub, M. C.; Murakami Iha, N. Y.; Meyer, T. J. *ChemSusChem* **2011**, *4*, 216−227.
(45) Song, W.; Brennaman, M. K.; Concepcion, J. J.; Jurss, J. W.; Hoertz, P. G.; Luo, H.; Chen, C.; Hanson, K.; Meyer, T. J. *J. Phys. Chem. C* **2011**, *115*, 7081−7091.
(46) Sekizawa, K.; Maeda, K.; Domen, K.; Koike, K.; Ishitani, O. *J. Am. Chem. Soc.* **2013**, *135*, 4596−4599.
(47) Chen, D. T.; De, R.; Mohler, D. L. *Synthesis-Stuttgart* **2009**, 211−216.
(48) Jurss, J. W.; Concepcion, J. C.; Norris, M. R.; Templeton, J. L.; Meyer, T. J. *Inorg. Chem.* **2010**, *49*, 3980−3982.
(49) Suzuki, K.; Kobayashi, A.; Kaneko, S.; Takehira, K.; Yoshihara, T.; Ishida, H.; Shiina, Y.; Oishi, S.; Tobita, S. *Phys. Chem. Chem. Phys.* **2009**, *11*, 9850−9860.
(50) Sasai, R.; Iyi, N.; Kusumoto, H. *Bull. Chem. Soc. Jpn.* **2011**, *84*, 562−568.
(51) Yamanaka, K.-i.; Okada, T.; Goto, Y.; Tani, T.; Inagaki, S. *Phys. Chem. Chem. Phys.* **2010**, *12*, 11688−11696.